Clays and Clay Minerals, Vol. 28, No. 4, 241–254, 1980.

KAOLINITE, SMECTITE, AND K-RECTORITE IN BENTONITES: RELATION TO COAL RANK AT TULAMEEN, BRITISH COLUMBIA

D. R. PEVEAR[1], V. E. WILLIAMS[2], AND G. E. MUSTOE[1]

Abstract—The Tulameen coal field is part of an Eocene nonmarine basin which received extensive volcaniclastic sediments due to its location within an active magmatic arc. Bentonite partings in the coal originally consisted of glassy rhyolitic tephra with phenocrysts of sanidine, biotite, and quartz. During the initial alteration, which took place within the swamp or shortly after burial, glass was transformed to either smectite-cristobalite-clinoptilolite or to smectite-kaolinite. The formation of kaolinite depended on the degree of leaching of silica and alkalies in the swamp environment. Some beds are nearly 100% kaolinite and can be designated as tonsteins. The smectite shows no evidence of interlayering; the kaolinite is well ordered. During alteration, sodium, originally a component of the glass, was lost from the system.

A later thermal event, which affected only the southern part of the basin, metamorphosed the smectite to a regularly interstratified illite/smectite with 55% illite layers and rectorite-type superlattice (IS-type). The source of potassium was dissolution of sanidine. Vitrinite reflectance measurements of the coal suggest that the smectite was stable to 145–160°C, at which temperature it transformed to K-rectorite.

The absence of randomly interstratified intermediates, even in beds rich in potassium, suggests that the transformation of smectite to K-rectorite was controlled by a steep thermal gradient possibly resulting from local magmatism or circulating geothermal fluids.

Key Words—Bentonite, Coal rank, Kaolinite, Mixed layer, Rectorite, Smectite, Tonstein, Vitrinite, Zeolite.

INTRODUCTION

The Tulameen coal field is one of several early Tertiary basins in south-central British Columbia that contain thick nonmarine sequences of coal-bearing sedimentary rocks rich in volcaniclastics (Figure 1). During Eocene time this area was an active magmatic arc east of a continental margin subduction zone (Dickinson, 1979). Volcanism and associated north–south trending normal faults (Davis, 1977; Okulitch *et al.*, 1977) blocked streams and created local basins in which peat and volcaniclastics accumulated. At Tulameen these volcaniclastics consist, in part, of thin, air-fall tephra layers interbedded with coal. The tephra layers have been altered to smectite, kaolinite, clinoptilolite, cristobalite, and a regularly interstratified illite/smectite (K-rectorite) and are here called bentonites. This study relates the mineralogy of the bentonites to variations in coal rank and paleotemperature.

GEOLOGIC SETTING

The stratigraphic relations and geologic setting of Tulameen have been summarized by Williams and Ross (1979); much of the following is taken from their report. The coals are part of the Allenby Formation which here is more than 800 m thick and consists (Figure 2) of a lower sandstone member, a middle coal-bearing member, and an upper sandstone member. A K-Ar date on biotite from bentonite just below the coal at Collins Gulch gave an age of 47 m.y. (Hills and Baadsgaard, 1967), which indicates that the Allenby Formation is Middle Eocene.

The lower member is 100–150 m thick and consists of sandstone, siltstone, shale, and tephra, with several thin andesitic flows near the base. The middle member is ~130 m thick and consists of shale, thin sandstone beds, and coal. The upper member is primarily coarse arkosic sandstone and conglomerate and is >600 m thick. The Allenby Formation overlaps the basal volcanic unit of the Princeton Group or lies unconformably on the Triassic Nicola Group and is unconformably overlain by Miocene-Pliocene flood basalts. Although the maximum depth to which the middle member of the Allenby Formation was buried is difficult to estimate, the reported thickness of overlying sediments suggests that it was at least 600 m and probably never much more than 1000 m. The Tulameen coal field is part of a southeast-plunging synclinal basin ~5 km long and 3 km wide (Figure 3). Beds dip from 25° to 65°; the southern part of the syncline is offset slightly by several faults.

The coal-bearing, 130-m thick middle member of the Allenby Formation consists of bentonitic shales and mudstones, thin sandstones, and several coal seams. The uppermost and thickest coal seam (the main coal seam) is 15–20 m thick over most of the basin and thickens to ~40 m to the south, possibly due to low-angle and bedding-plane thrust faults. Interbedded with the

[1] Department of Geology, Western Washington University, Bellingham, Washington, 98225.
[2] Department of Geology, University of British Columbia, Vancouver, British Columbia V6T 1W5, Canada.

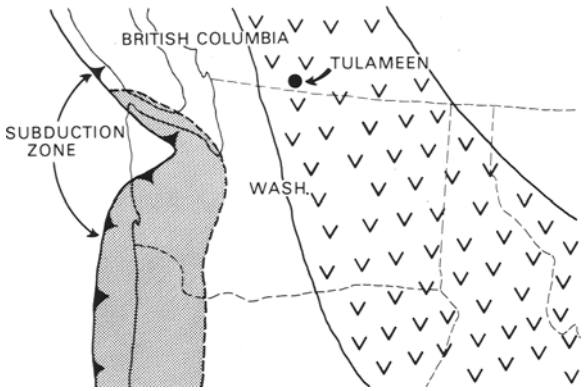

Figure 1. Index map showing location of Tulameen Basin and Eocene paleogeography (from Dickinson, 1979). Stippled areas are marine basins; area with check pattern is magmatic arc.

main seam are numerous beds of cream-colored bentonite which are the subject of the present study. These beds vary from a few millimeters to 50 cm in thickness. Maceral analyses (Williams, 1978) show the main-seam coals to consist of more than 90% vitrinite, which suggests a large contribution from woody plant material; therefore, a forest–moor environment is indicated.

SAMPLES AND METHODS

Samples

More than 100 samples of bentonite partings from the main coal seam were examined by X-ray powder diffraction (XRD), scanning electron microscopy (SEM), and optical microscopy. Sample collecting sites, consisting of trenches, diamond drill holes, and an open pit mine, are shown on Figure 3. Representative analyses are shown in Table 1. Sample prefixes are from Figure 3, and samples are arranged in normal stratigraphic sequence. For a more detailed description of the individual stratigraphic sections and sample locations, see Williams (1978).

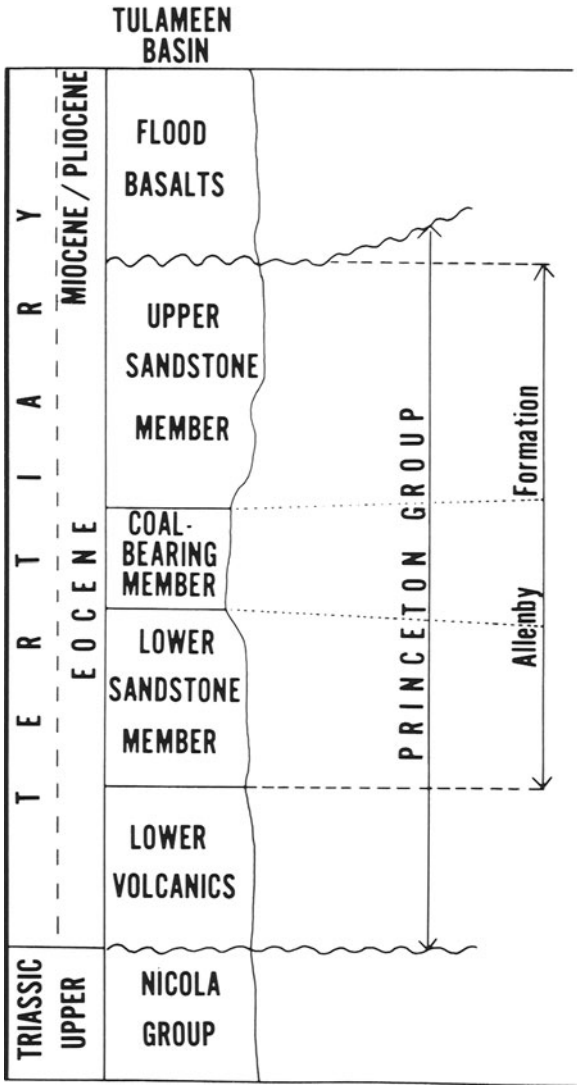

Figure 2. Diagrammatic stratigraphic section of Tulameen Basin; not to scale (from Williams, 1978).

Methods

About twenty thin sections were prepared for optical microscopic examination from the better-indurated specimens; most samples, however, were too unconsolidated to be sliced and ground.

Whole rock and clay (<2 μm) fractions of more than 100 samples were examined by XRD techniques with a GE XRD-5 apparatus, using Ni-filtered CuKα radiation and a scanning rate of 2°2θ/min. Whole rock samples were ground in a ball mill, sieved through a 100-μm nylon screen, and pressed into side-loading, plastic sample holders. XRD scans from 2° to 65°2θ were made. Clay (<2 μm) fractions were separated by ultrasonic disaggregation in distilled water and centrifugation, either with a standard centrifuge or a Sharples supercentrifuge, using time and speed conditions of Jackson (1974). The clay suspension was then sucked through a porous ceramic tile to produce an oriented aggregate diffraction mount. Each specimen was saturated with Mg by sucking 2 N $MgCl_2$ through the specimen, followed by distilled water. Oriented specimens were scanned from 2° to 35°2θ under the following conditions: (1) air dry (untreated); (2) heated to 300° and 550°C for 1 hr or longer; and (3) solvated with ethylene glycol.

Rock chips were cemented onto aluminum stubs, sputter-coated with a Au-Pd alloy, and examined with an AMR scanning electron microscope at 25 kV.

Elemental analyses of nine whole-rock and one clay-size samples of bentonites are given in Table 3. All

https://doi.org/10.1346/CCMN.1980.0280401 Published online by Cambridge University Press

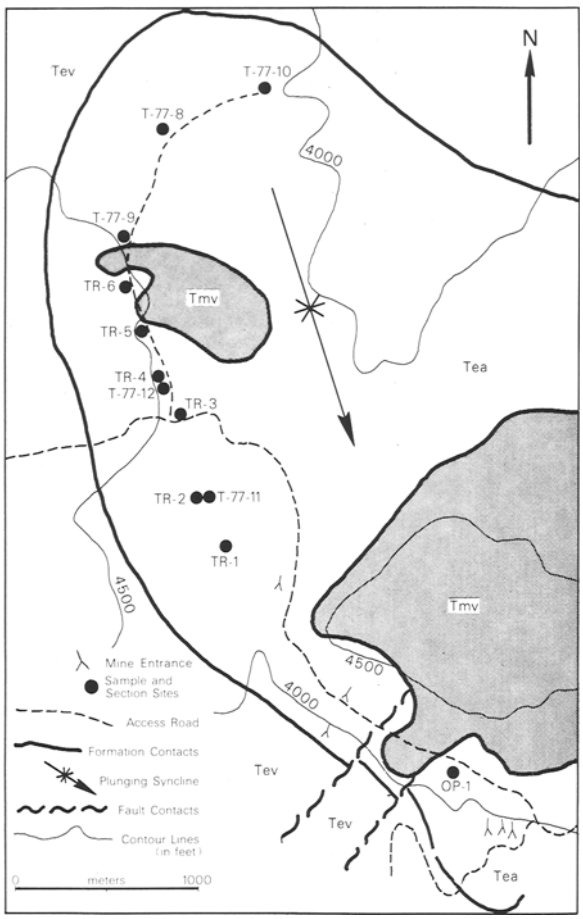

Figure 3. Geologic map of Tulameen Basin showing sample sites. T = drill hole, TR = trench, OP = open pit mine, Tmv = Miocene basalts, Tea = Eocene Allenby Formation, Tev = Eocene volcanics of the Princeton Group (from Williams, 1978).

elements were analyzed by atomic absorption spectrophotometry using the lithium metaborate fusion technique. Silicate rock standards of similar composition were used to standardize the method. Each reported analysis is an average of two.

MINERALOGICAL RESULTS

Whole-rock petrography

In thin section the samples consist of highly angular, sand-size fragments of quartz, sanidine, and biotite in a fine-grained matrix of quartz, clay, and other minerals. Relict glass shards, now altered to quartz and clay minerals, were clearly visible in some specimens where they constitute the entire matrix. Some samples contain fresh biotite, but in others the biotite is partially or completely altered and has expanded to a vermicular material of low birefringence, possibly kaolinite.

Sanidine

Sanidine is a minor constituent of many whole-rock samples and is a major constituent of a few; it is rare in the clay fractions. For those samples with sufficient diffraction maxima, the "three peak" method of Wright (1968) showed the sanidine to be monoclinic high sanidine. Some samples, particularly those from trench 1, contain sanidine in the clay fraction; SEM photos of one of these (Figure 4a) show an abundance of euhedral sanidine crystals 1–6 μm in size. These may be authigenic, since their morphology is distinct from the cleavage fragments of phenocrystic sanidine present in the same sample. They also appear to be monoclinic high sanidine, but this is uncertain because they could not be separated from the phenocrystic sanidine for analysis.

Quartz

Quartz is a major or minor constituent of most of the whole-rock samples, but it is rare in the clay fractions.

Cristobalite

Low cristobalite is present in some samples, both in the whole-rock and clay fractions, and is a major constituent of a few samples. A broad peak at 4.06 Å was generally the only peak seen, but in some samples peaks were also observed at 3.13, 2.85, and 2.49 Å. This material resembles that described by Jones and Segnit (1971) as opal-C; it cannot be opal-CT, as no tridymite peaks were observed. The distinctive lepisphere morphology of opal-CT described by Hein *et al.* (1978) and others was not seen in any of the Tulameen samples.

Clinoptilolite

Zeolite is a minor constituent in both whole-rock and clay-size fractions of 11 samples, but only in three samples were sufficient diffraction peaks present to permit identification as a member of the clinoptilolite/heulandite group. The peak most commonly observed was at ~9.02 Å, but as many as 7 additional maxima were seen in some samples. The peaks persisted after heating to 500°C which is diagnostic of clinoptilolite (Mumpton, 1960).

Smectite

Smectite is a major constituent in whole-rock and clay fractions of 51 samples. A typical diffraction pattern is shown in Figure 5. Ethylene glycol solvation expands the smectite to about 17 Å and produces an integral series of higher-order reflections which indicate complete absence of non-expanding interlayers in all samples. The 060 reflection at 1.49 Å in randomly oriented specimens shows the smectite to be dioctahedral. Cation-exchange analysis of several samples (none of which were pure smectite) show the major exchangeable cations to be Ca and Mg (see Table 3).

https://doi.org/10.1346/CCMN.1980.0280401 Published online by Cambridge University Press

Table 1. Mineral content of Tulameen bentonites as determined by X-ray powder diffraction.

Sample number	Q	C	S	Sm	K-R	K	Other	Assemblage
TR-6-72-1	m–		m–	MM		MM		II
TR-6-60-1	M–			–M		–m		II
TR-6-57-1	m–		t–	MM		MM		II
TR-6-47-1	M–		tt	mm		MM		II
TR-6-44-1	m–		t–	MM		tm		II
TR-6-42-1	MM		mm			tm		?
TR-6-40-1	M–			MM		MM		II
TR-6-36-1	M–		tt		–m	MM		III
TR-6-32-1	M–		t–	tm	–m	MM		?
TR-6-8-1	m–			MM		MM		II
TR-6-0-1	m*		t*	M*		t*		II
TR-4-70-3	m–	mt		MM			cp	I
TR-4-70-2	MM	m–	mm	m–				I
TR-4-70-1	m–	Mm	m–	MM			cp	I
TR-4-60-1	m–			MM		–m		II
TR-4-45-1	M–	m–	m–	MM		mM		I?
TR-4-41-3	m–	Mt	M–	MM			cp	I
TR-4-41-1	m–	mm	t–	MM				I
TR-4-36-1	M–		MM	m–		tM		II
TR-4-34-1	m–		t–	mm		MM		II
TR-4-33-1	M–			Mm		MM		II
TR-4-32-1	Mm		mm	t		–M		II
TR-4-28-1	m–			MM		tm		II
TR-4-26-1		*t		*M				I
TR-4-20-1	t–			MM		mm		II
TR-4-18-1				MM				I
TR-4-14-1	mm		tt	mm	–m	MM		?
TR-4-9-1	m–			MM		mt		II
T-77-12-99.4	m–	Mm	m–	MM			cp, mi	I
T-77-12-103.6		Mm		MM				I
T-77-12-112.2	m–	Mm	t–	MM				I
T-77-12-119.2	m–	mt	t–	M–			cp, mi	I
T-77-11-98.2	m–	Mt	m–	MM			cp, mi	I
T-77-11-102.1	t–	Mm		MM			cp	I
T-77-11-105.2				MM				I
TR-1-79-10	M–		–t			mM		?
TR-1-79-9	m–		mm		tt	MM		III
TR-1-79-8	m–		m–		–t	MM		III
TR-1-79-7	M–		m–		mm	MM		III
TR-1-79-6	M–		m–		mm	MM		III
TR-1-79-5	M–		mt		–m	tM		III
TR-1-79-4	M–		m–		–m	mM		III
TR-1-79-3	M–		MM			tm	mi	?
TR-1-X-J	m–	Mt	t–	MM		–t	cp, mi	I
TR-1-X-B				*t		*M		II
TR-1-IX-F	M–				MM	MM		III
TR-1-IX-C					*t	*M		III
TR-1-IX-B	M–				mM	mM		III
TR-1-VIII-H	M–		m–		tm	MM		III
TR-1-VIII-G	M–		t–		tt	MM		III
TR-1-VIII-E	M–		m–		mm	MM		III
TR-1-VIII-A	M–			MM	–t	tM		?
TR-1-VII-H	M–			MM		tt		II
TR-1-VII-F	M–			MM		mM		II
TR-1-VII-A				*m	*m	*M		?
TR-1-VI-E	m–		t–	MM		Mm		II
TR-1-VI-A	M–		m–	tm		mM		II
TR-1-V-D	m–			MM		mm		II
TR-1-V-C	M–		m–	MM		Mm		II
TR-1-V-A				*M		*t		II
TR-1-IV-D				*M		*m		II
TR-1-IV-C				*M				II
TR-1-IV-B				*M				II
TR-1-III-C				*t		*M		II

https://doi.org/10.1346/CCMN.1980.0280401 Published online by Cambridge University Press

Table 1. Continued.

Sample number	Q	C	S	Sm	K-R	K	Other	Assemblage
TR-1-9-1				*m		*M		II
TR-1-0-D				*m		*M		II
OP-79-13	M–				–M	tM		III
OP-79-12	m–					–t	sd	III?
OP-79-11	M–		–t		mM	mM		III
OP-79-10			*t		*M	*m		III
OP-79-9	M*		t*		M*	t*		III
OP-79-8	M–		t–		MM	tm		III
OP-79-7			–t		–m	tM	sd	III
OP-79-6					–m	mM	sd	III
OP-79-5	M–				MM			III
OP-79-4	M–				tM	–t	sd	III
OP-79-3	M–				MM	tm		III
OP-79-2	M–				MM	–t		III
OP-79-1	M–				MM	mt		III

Q = quartz, C = low cristobalite, S = sanidine, Sm = smectite, K-R = K-rectorite, K = kaolinite, M = major constituent, m = minor constituent, t = trace constituent. The abundance symbols are arranged in pairs; the first letter refers to the whole rock, the second letter refers to the <2-μm fraction; a dash preceding or following a single abundance symbol indicates that the mineral is absent from the specified fraction; an asterisk preceding or following a single abundance symbol indicates that the specified fraction was not analyzed. Other = other minerals present, including: mi = mica, cp = clinoptilolite, sd = siderite; assemblage = mineral assemblages described in text. Sample prefixes refer to sampling sites shown on Figure 3; samples are arranged in normal stratigraphic sequence.

K-rectorite

A large number of the bentonite samples contain regularly interstratified illite/smectite here called K-rectorite (Eberl, 1978a). Randomly interstratified species were not observed. In thin section this mineral can be seen to have replaced original glass shards. SEM photos (Figure 4b) show irregular plates ~0.1 μm thick and up to 2 μm across with serrated edges. Some show crude hexagonal outlines.

XRD patterns of the K-rectorite are shown in Figure 6. Comparison with data of Reynolds and Hower (1970) shows this mineral to be a regularly interstratified illite/smectite with IS order and 55% illite layers. Środoń's methods (1980) give ~60% illite layers. IS order (also called allevardite or rectorite-type) implies regular alternation of illite and smectite layers with any extra illite randomly dispersed between ordered packets.

The XRD pattern of the 550°C-treated sample (Figure 6) shows a small shoulder near 24 Å and the principal peak at 10.3 Å, having failed to collapse to the expected 10 Å. These features persisted even when the sample was heated to 650° for 12 hr, suggesting the presence of <10% regularly interstratified chlorite layers or hydroxy-aluminum interlayers. Judging from its large Al content (Table 3, OP-79-2), the chlorite may be dioctahedral.

Data from a different specimen with XRD properties nearly identical with those in Figure 6 were analyzed by the direct Fourier transform method of MacEwan (1956); the results are shown in Figure 7, and the data upon which this figure is based are given in Table 2. Eight diffraction maxima from an ethylene glycol-treated oriented mount were utilized. The layer transform (G) was calculated from the dioctahedral silicate skeleton as modeled by Reynolds (1967); single crystal Lorentz-polarization factors were used. The direct Fourier transform gives a useful structural analysis as long as both types of layers have similar composition and therefore similar layer transforms. Given the highly aluminous nature of this clay, the layers cannot be of very different compositions. The function W(R) is the probability of finding a given spacing, R, in the crystal; the peaks on Figure 7 indicate interlayer spacings which are abundant.

The baseline on Figure 7 was adjusted so that the observed heights of the fundamental spacings at 10 Å (I = illite) and 17 Å (S = ethylene glycol-smectite) are 0.55 and 0.45, respectively; therefore, there are 55% illite layers. The calculated height was computed on the basis of these fundamental probabilities and with the constraint that no two smectite layers occur in contact—that is, the probability of a smectite–smectite pair is zero. When illite is more abundant than smectite, this is the condition for the IS type of superlattice ordering described by Reynolds and Hower (1970). With the single exception of the peak at 47 Å, the observed and calculated probabilities agree quite well, which suggests that the simple model described above is valid for the Tulameen K-rectorite. The lack of agreement at 47 Å may indicate an increased tendency to form three illite layers between smectite—the ISII or Kalkberg-type superlattice of Reynolds and Hower (1970). The small

https://doi.org/10.1346/CCMN.1980.0280401 Published online by Cambridge University Press

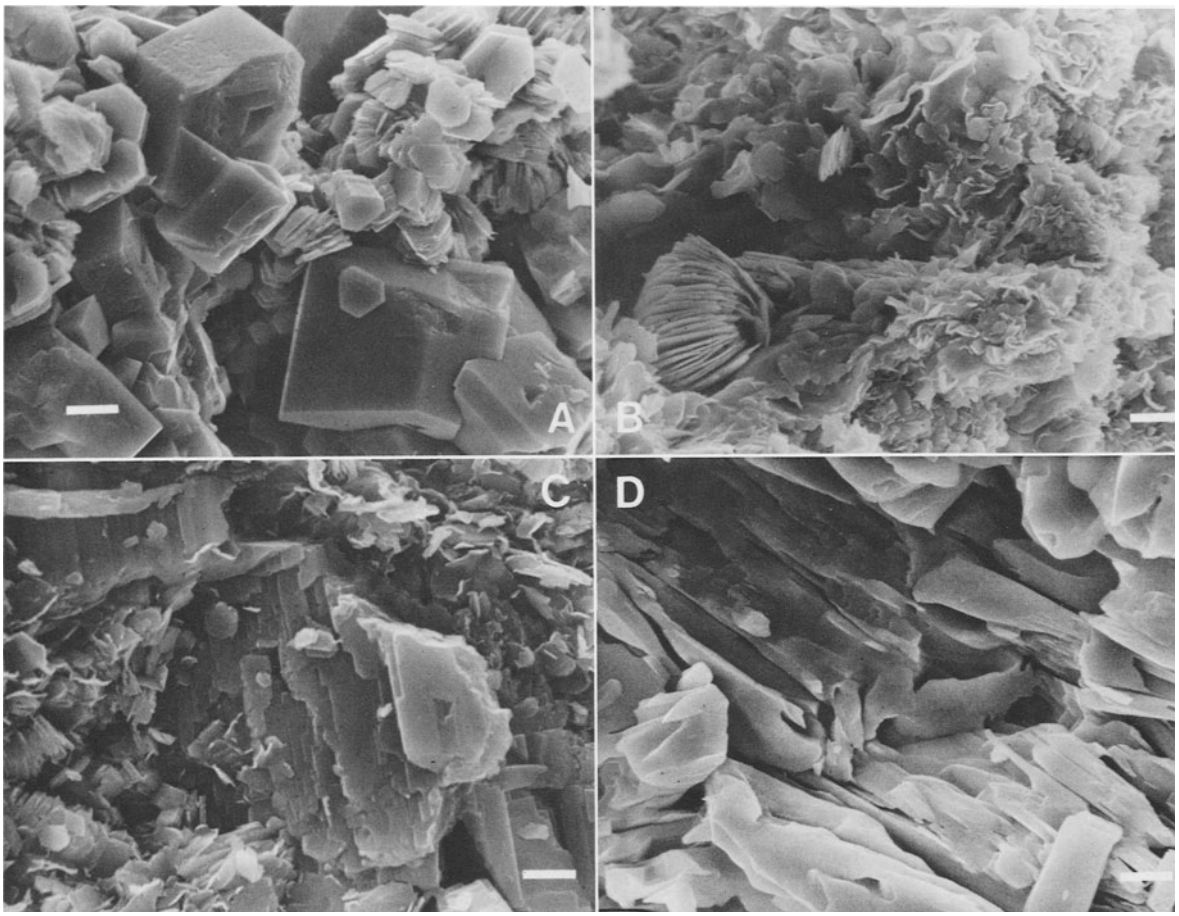

Figure 4. Scanning electron micrographs of Tulameen bentonites; bar scale is 2 μm. a. Authigenic (?) K-feldspar with hexagonal plates of kaolinite; sample TR-1-79-4. b. K-rectorite, vermicular aggregate may be kaolinite; sample OP-79-2. c. Sanidine showing possible solution features, with K-rectorite and kaolinite; sample TR-1-79-7. d. Solution fluting in sanidine; sample TR-4-70-1.

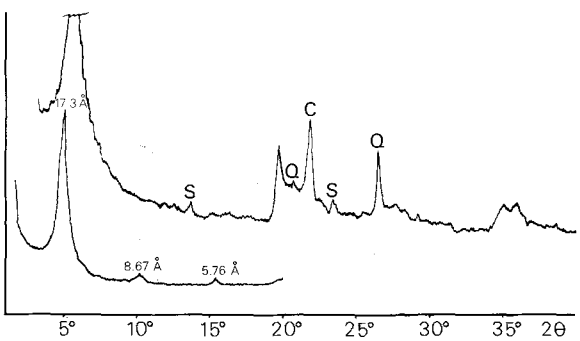

Figure 5. X-ray powder diffraction patterns of Tulameen smectite (assemblage I); also present are sanidine (S), quartz (Q), and cristobalite (C); all other peaks are due to smectite; upper pattern is a random bulk rock sample; lower pattern is an oriented <2-μm, ethylene glycol-treated sample; CuKα radiation.

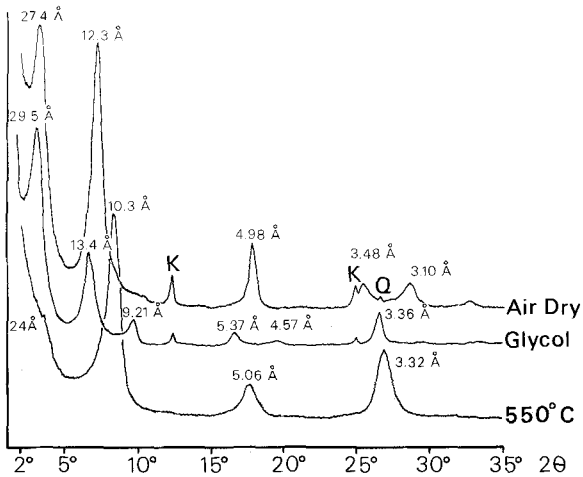

Figure 6. X-ray powder diffraction patterns of oriented specimens of K-rectorite (assemblage III): also present are kaolinite (K) and quartz (Q); CuKα radiation.

https://doi.org/10.1346/CCMN.1980.0280401 Published online by Cambridge University Press

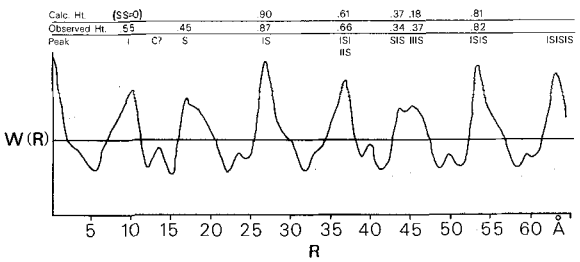

Figure 7. MacEwan direct Fourier transform of K-rectorite; data for transform are in Table 2; explanation is in text.

peak near 14 Å (C?) suggests a possible chlorite component.

Figure 8 shows the pattern of an ethylene glycol-treated sample of the same specimen shown in Figure 6, and a pattern calculated by a modified version of a computer program (MOD 4) written by R. C. Reynolds and based on methods described in Reynolds (1967). The computer profile is based on the probability conditions previously described for IS order, 55% illite layers, and diffracting domains (N) 4–8 layers thick. Agreement in peak position, intensity, and shape appears good except near 29 Å. This discrepancy may be due to instrumental factors affecting peak positions at very low angles.

A chemical analysis of the 2–0.2-μm fraction of nearly pure K-rectorite is given in Table 3 (OP-79-2); a structural formula cast from this analysis is shown below.

$$[(Al_{1.90}Fe^{+3}_{0.01}Fe^{+2}_{0.03}Mg_{0.05})_{1.99}(Si_{3.57}Al_{0.43})O_{10}(OH)_2]^{-0.54}$$
$$[Ca_{0.04}Mg_{0.03}Na_{0.01}K_{0.38}]^{+0.53}$$

The formula is reasonable for the K-rectorite described from the diffraction data, but little can be deduced concerning the composition of the component layers.

Kaolinite

Kaolinite makes up more than 25% of many of the whole-rock samples and is even more abundant in the clay-size fraction. A few of the beds consist almost

Table 2. Data for MacEwan transform in Figure 7.

°2θ	I_s[1]	G[2]
3.0	920	154.0
6.5	440	87.5
9.7	65	14.9
16.4	50	−46.9
19.6	15	−20.4
26.5	120	55.9
33.3	10	34.4
43.7	10	−49.3

[1] I_s = peak intensity (cps).
[2] G = layer transform.

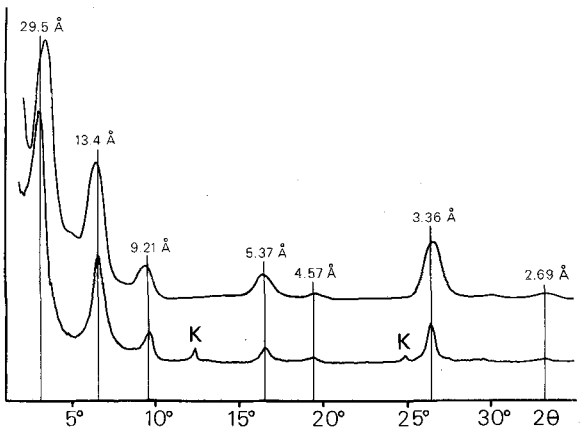

Figure 8. Actual (lower pattern) and calculated (upper pattern) X-ray powder diffraction patterns of ethylene glycol-treated, oriented K-rectorite; calculated pattern is by the methods of Reynolds (1967), using 55% illite layers, maximum IS-type order, and diffracting domains (N) 4–8 layers thick; K = kaolinite; CuKα radiation.

entirely of kaolinite, with minor quartz and sanidine. Figure 4a shows the typical appearance of Tulameen kaolinite under the SEM. Crystals are generally well-formed hexagonal plates 1–3 μm across in short stacks or in long vermicular aggregates; a loose, open packing of the plates is characteristic. A diffraction pattern for the kaolinite is shown in Figure 9, which is a whole rock analysis of a randomly oriented sample. All unlabeled peaks are due to kaolinite, which is well ordered as evidenced by the clearly resolved, non-basal reflections near 20°2θ and also between 35° and 40°2θ. There is no evidence of dickite or nacrite. A few samples were treated with DMSO and showed expansion to 11.2 Å, typical for kaolinite. All kaolinite peaks vanished upon heating to 550°C.

DISCUSSION OF MINERALOGY

Origin

The mineralogy and petrology of the Tulameen bentonites suggest that they formed by alteration of glassy rhyolitic tephra containing quartz, sanidine, and biotite phenocrysts; all other minerals are postulated to have formed by alteration of glass shards. Detrital components of non-tephra origin appear to be absent; indeed, the low energy swamp environment of deposition would tend to exclude such a possibility. The overlying upper sandstone member of the Allenby Formation contains abundant microcline perthite of obvious detrital origin, yet this mineral was not observed in the bentonites.

Mineral assemblages

Most of the samples examined can be placed in one of the following mineral assemblages:

https://doi.org/10.1346/CCMN.1980.0280401 Published online by Cambridge University Press

I. smectite + low cristobalite ± zeolite ± (sanidine, biotite, quartz)
II. smectite + kaolinite + quartz ± (sanidine, biotite)
III. K-rectorite + kaolinite + quartz ± K-feldspar ± siderite ± (sanidine, biotite).

Because all of the above assemblages contain phenocrystic sanidine, quartz, and biotite, the principal differences are in the nature of the fine-grained constituents. Only 7 of more than 100 analyzed samples fail to fit into one of these three assemblages, including samples TR-1-79-3, TR-6-42-1, and TR-1-79-10 which contain neither smectite nor K-rectorite and therefore fit neither assemblage II nor III, and samples TR-6-32-1, TR-4-14-1, TR-1-VIII-A, and TR-1-VII-A which contain both K-rectorite and smectite and therefore fit none of the assemblages.

The relation of the assemblages to stratigraphy and structure within the Tulameen basin is complicated by the difficulty of correlating individual bentonite beds between the sample sites shown on Figure 3. This difficulty is at least in part due to the presence of low-angle and bedding-plane thrust faults. In spite of this difficulty, some regional relationships clearly stand out (Figure 10). All samples in the northern part of the basin belong to assemblage I or II with the exception of one sample in trench 6 which is in assemblage III. Therefore, the northern samples contain either smectite + cristobalite ± clinoptilolite or smectite + kaolinite. Samples from the southern part of the basin belong to either assemblage II or III. The samples from trench 1 fit assemblage II in the lower part of the section and assemblage III in the upper part, with one exceptional sample belonging to assemblage I. All samples from the open pit (Blakeburn pit) fit assemblage III. Therefore, the K-rectorite-bearing samples are all from the southern part of the basin.

Variations in mineralogy within individual bentonite beds were generally not ascertained, but all 5 samples collected across a 50-cm thick bentonite from the open pit (OP-79-1 to OP-79-5) are nearly identical.

The mineral variations observed in the Tulameen bentonites could have one or more of the following origins: (1) differences in original chemical composition of the tephra, (2) additions of detrital material, (3) reactions at low temperature with swamp and groundwaters relatively soon after deposition, and (4) thermal or hydrothermal metamorphism at an undetermined time after deposition. Each of the three assemblages is discussed below with respect to the possible origins listed above.

Assemblage I. Assemblage I (smectite + cristobalite ± clinoptilolite) is widely reported as the first alteration stage of glassy silicic tephra in a number of geologic environments (Hay, 1978; Iijima, 1978; Deffeyes, 1959; Reynolds and Anderson, 1967; Murata and Whiteley, 1973; Bramlette and Posnjak, 1933). According to Hay (1978), this reaction can take place during the first 1000 years after deposition. Murata and Whiteley (1973) suggested that clinoptilolite in young deep sea sediments formed at 10°C. Although low cristobalite has also generally been described as originating from alteration of glass at low temperature, the oxygen isotope data of Henderson *et al.* (1971) suggest its derivation from biogenic silica.

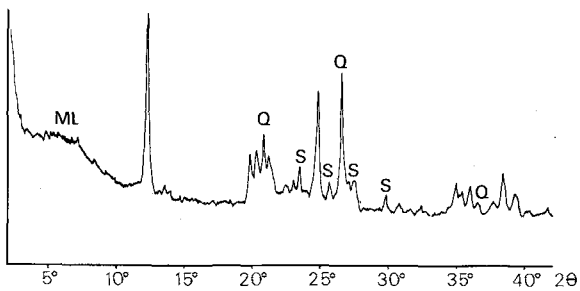

Figure 9. X-ray powder diffraction pattern of bulk sample of Tulameen kaolinitic bentonite (TR-1-79-8) (assemblage III); random orientation; ML = mixed layer (rectorite), Q = quartz, S = sanidine; all other major peaks are due to kaolinite; CuKα radiation.

The first three analyses in Table 3 are of assemblage I bentonites, each of which contains major smectite and cristobalite and minor clinoptilolite. Biotite in these samples is generally fresh and unaltered compared with that in other assemblages. The high silica values reflect the content of cristobalite, smectite, and phenocrystic quartz; the high potash values reflect the abundance of sanidine phenocrysts. Assemblage I samples represent tephras that are less altered than other assemblages and most similar in chemical composition to the original tephra. Comparison with data from unaltered silicic pyroclastics (Mueller and Saxena, 1977) shows the compositions of these three bentonites to be nearly identical with those of rhyolite tuffs and obsidians with one major exception: fresh tuffs contain ~4.0% Na_2O, whereas the bentonites contain only ~0.30%. It is suggested that sodium was originally present in the glass component of the Tulameen tephra, and that subsequent alteration of the glass released sodium which was lost from the system. K, however, was originally present in the more stable sanidine phenocrysts and was retained.

Assemblage I bentonites were altered relatively soon after deposition and at low temperature by reaction of pore waters with glassy rhyolitic tephra. If Na was lost, the system could not have been entirely closed. Hills and Baadsgaard (1967) reported fresh glass in tephra (not interbedded with coal) from southern British Columbia that is correlative with the Allenby Formation;

https://doi.org/10.1346/CCMN.1980.0280401 Published online by Cambridge University Press

Table 3. Chemical analyses of bentonites from Tulameen, British Columbia.[1]

	TR-4-41-3 (I)	TR-4-70-1 (I)	T-77-12-99.4 (I)	TR-6-72-1 (II)	TR-1-V-C (II)	TR-1-VI-E (II)	TR-1-IX-F (III)	TR-1-79-7 (III)	OP-79-1 (III)	OP-79-2[2] (III)
SiO_2	70.69	71.33	68.77	51.96	55.65	54.48	55.27	65.00	71.84	52.62
Al_2O_3	14.33	14.23	14.22	28.50	25.35	26.02	28.51	21.66	15.98	29.08
TiO_2	.05	.05	.05	.58	.73	.53	.36	.05	.21	.12
Fe_2O_3[3]	1.48	1.53	1.34	1.51	1.13	1.52	1.41	1.04	.56	.75[4]
MgO	.49	.47	.55	.51	.80	.75	.49	.19	.50	.77
Na_2O	.25	.27	.40	.18	.09	.27	.07	.31	.10	.10
K_2O	4.24	4.01	3.33	2.18	2.66	1.55	1.60	3.58	2.51	4.44
CaO	.58	.54	1.57	.19	.41	.60	.19	.17	.32	.51
MnO	.01	.01	.01	.01	.01	.01	.01	.01	.04	.06
H_2O-	4.00	4.00	5.30	4.30	6.00	6.60	3.50	1.40	4.30	6.25
H_2O+	3.82	3.51	4.53	10.30	7.55	8.10	8.68	6.59	3.71	5.52
Total	99.94	99.96	100.07	100.22	100.38	100.43	100.09	100.00	100.07	100.22

[1] Roman numerals = mineral assemblage.
[2] <2-μm fraction.
[3] Total Fe calculated as Fe_2O_3.
[4] FeO = 0.52, Fe_2O_3 = 0.19.

Exchangeable cations (meq/100 g clay) T-77-12-99.4 = 0.10 Na, 2.80 K, 56.10 Ca, 12.20 Mg (Total = 71.20). OP-79-1 = 0.00 Na, 2.00 K, 32.60 Ca, 21.20 Mg (Total = 55.80).

therefore some unspecified conditions in the depositional or post-depositional environment must have produced the Tulameen bentonites, which contain no unaltered glass.

Assemblage II. The three analyses of assemblage II bentonites listed in Table 3 are from samples containing major kaolinite and smectite and minor quartz and sanidine. This assemblage differs from assemblage I in having kaolinite and lacking cristobalite or zeolite. Assemblage II bentonites range from those with major kaolinite and traces of smectite to those with major smectite and traces of kaolinite. The high Al_2O_3 and low SiO_2 and alkali contents of these samples as compared to those of assemblage I suggest that assemblage II could have been produced by leaching of silica and alkalies from material with an initial composition similar to assemblage I. Theoretical activity diagrams such as those of Helgeson *et al.* (1969) and Davies *et al.* (1979) allow the coexistance of zeolite-smectite or smectite-kaolinite, but not zeolite-kaolinite. The pair kaolinite-cristobalite is also never found at Tulameen; evidently the cristobalite or its precursor is removed by leaching in the swamp environment. Similar cristobalite relations were reported by the first author of this report in an unpublished study of bentonite partings in coals of the Centralia–Chehalis basin of southwest Washington, where partings belong either to a kaolinite-smectite or a cristobalite-smectite assemblage.

It is also possible that the kaolinite was added to the tephra as a detrital component washed into the swamp from low-lying, saprolitically weathered hills surrounding the basin. Horton (1978) demonstrated such an origin for deposits of b-axis-disordered kaolinite interbedded with coal in southwestern British Columbia. Saprolitic paleosols containing kaolinite are considered to have formed in a warm to subtropical climate, similar to that suggested to have occurred in this area during middle Eocene time (Thompson *et al.*, 1978; Williams and Ross, 1979), so this idea is not without merit. Because the Tulameen kaolinite is well ordered and occurs as euhedral crystals and delicate vermicular aggregates that show no evidence of transport, its detrital origin is ruled out.

The assemblage II analyses in Table 3 are similar to analyses which Spears and Kanaris-Sotiriou (1979) reported for British and European tonsteins (kaolinitic clayrocks interbedded with coal). There has long been a controversy concerning the origin of tonstein, particularly as to its volcanic parentage (Spears and Kanaris-Sotiriou, 1979; Loughnan, 1978). The complete gradation from smectite-rich beds to nearly pure kaolinite in the Tulameen bentonites suggests that at least some tonsteins are volcanic, as was concluded by Bohor *et al.* (1978) for tonsteins in Cretaceous and Tertiary coals of the Rocky Mountains.

Assemblage II bentonites formed by leaching in the acid swamp environment of silica and alkalies from material of initial chemical composition similar to assemblage I. Hoffman and Hower (1979) described the same mode of origin for minor kaolinite in bentonites of the Montana disturbed belt. What is not clear is whether the reaction steps were: glass → I → II, or glass → II, and whether the reaction actually took place in the swamp, or after burial in the presence of groundwater or formation water. Because silicified deposits or veins of opal and chalcedony have not been found in close proximity, it is concluded that the variable amount of kaolinite in the bentonites is the result of exposure to variable degrees of leaching in the swamp environment itself, and that assemblages I and II were formed under otherwise similar conditions.

Assemblage III. Assemblage III is typified by K-rectorite and kaolinite and the absence of smectite; it occurs in the southern part of the Tulameen basin. The 3 whole-rock analyses of assemblage III bentonites in Table 3 have a wide range which reflects large variations in mineral composition. Samples TR-1-IX-F and TR-1-79-7 contain large amounts of quartz and kaolinite as well as K-rectorite, and sample OP-79-1 contains major K-rectorite and quartz and traces of kaolinite; these variations are largely reflected in the SiO_2 and Al_2O_3 values in the analyses. The high K_2O in sample TR-1-79-7 is due to the presence of sanidine.

It is postulated that the K-rectorite of assemblage III was derived by metamorphism of assemblage I or II bentonites as a step in the sequence smectite → mixed layer clay → illite described by Dunoyer de Segonzac (1970) and Hoffman and Hower (1979), and as synthesized by Eberl (1978a). The presence of absence of K-rectorite cannot be easily attributed to differences in bulk chemical composition because all the bentonites in Table 4 have abundant K. It is assumed that during metamorphism the K and Al necessary to form K-rectorite were derived by solution of sanidine and perhaps biotite and potassic clinoptilolite. Figure 4c shows a sanidine grain with possible solution texture in contact with K-rectorite and kaolinite. Figure 4d shows a sanidine grain with pronounced solution fluting, very similar to that produced in hydrothermal experiments of Divis and McKenzie (1975). At Tulameen, unlike the Montana disturbed belt described by Hoffman and Hower (1979), the addition of K from outside the bentonite bed is not necessary for its transformation to K-rectorite.

The nature of the metamorphism at Tulameen is certainly different than the burial metamorphism described by Hower *et al.* (1976) and Hoffman and Hower (1979), wherein the proportion of randomly interstratified illite in smectite progressively increases over thousands of meters depth until, at a temperature near 100°C, an ordered structure forms. Tulameen bentonites contain either smectite with no interlayered illite (<10%) or K-rectorite; random interlayering was not observed. These differences are probably attributable to the presence of a much steeper thermal gradient at Tulameen, but the source of the heat is not known. Considering that the Tulameen basin is located within a magmatic arc that was active during and after deposition and that the basin was folded, faulted, and later covered by Miocene basalts, the heat source was probably magmatic, although the heat may have been transmitted a considerable distance by circulating geothermal fluids. That the overlying basalts were not the heat source is suggested by the presence of assemblage I and II bentonites only a few meters from an exposed contact with the basalt in trench 6.

In detail, the distribution of assemblage III bentonites is difficult to explain. In trench 1 the lower part of the section is in assemblage II, but the upper part is in assemblage III. The upper section here is highly fractured and faulted which suggests that the fractures provided ingress for hot fluids, or that the rocks were metamorphosed elsewhere and faulted into their present location. The transformation of smectite to rectorite could have been prevented, in some beds, by interlayer Ca (Eberl, 1978b), especially where a source of K (sanidine) was not available. In trench 5 all bentonites are in assemblage II except for one which is in assemblage III. This bed may be close to a bedding plane thrust fault, although evidence for such a fault was not found.

The absence of randomly interstratified intermediate phases suggests the direct transformation of either glass or smectite to K-rectorite, as does the coexistence of both smectite and K-rectorite, in four of the samples. In hydrothermal syntheses at 300°–400°C and of 30 days duration, Eberl (1978a) found that K-montmorillonite produced K-rectorite without evidence of random intermediate phases. From studies of the alteration of glassy silicic volcanics from drill holes in the Wairakei geothermal area, New Zealand, Steiner (1968) found that the alteration was more intense near fault zones and that mixed layering in the <10–65% illite range was absent. He observed either smectite or mixed-layer clays with 65% or more illite layers (at least some of which have rectorite ordering as determined by an examination of his data); as at Tulameen, intermediate phases were absent.

Where thermal gradients are steep, reaction times relatively short, and potassium readily available, the transformation of smectite to K-rectorite takes place without the formation of randomly interstratified intermediate phases. These criteria define the hydrothermal case as compared to the burial metamorphic case described above. It should be pointed out, however, that even in the burial metamorphic case the transformation to an ordered (rectorite) structure takes place over a relatively small stratigraphic interval where there is an abrupt change from ~25% randomly interlayered illite to ~60% illite and rectorite structure (Hower *et al.*, 1976).

All assemblage III samples contain at least traces of kaolinite, which is assumed to have largely formed early in the development of assemblage II. However, as shown by Hoffman and Hower (1979), where the amount of K is limited, the reaction to K-rectorite could take the form:

$$(1)\quad K^+ + \text{X-smectite} \rightarrow \text{K-rectorite} + \text{kaolinite} + \text{quartz} + X^+$$

rather than the form:

$$(2)\quad K^+ + \text{X-smectite} \rightarrow \text{K-rectorite} + \text{quartz} + X^+$$

https://doi.org/10.1346/CCMN.1980.0280401 Published online by Cambridge University Press

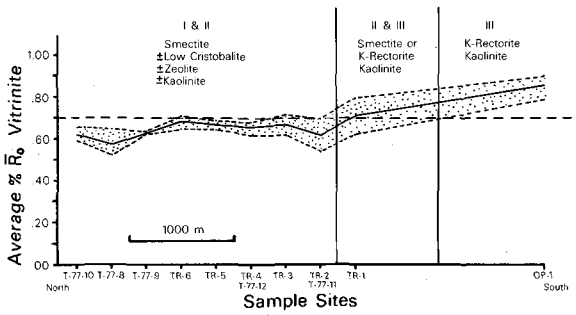

Figure 10. Plot of vitrinite reflectance ($\bar{R}_0$) vs. sample location; stippled area is the range of values, solid line is the mean. Horizontal scale is map distance between sample locations as shown on Figure 3. Dashed horizontal line is approximate % $\bar{R}_0$ value for the reaction smectite → K-rectorite.

where K is in excess. Because assemblage I bentonites (which lack kaolinite and contain sanidine) should be metamorphosed to kaolinite-free assemblages (reaction 2), and because all assemblage III samples contain kaolinite, it follows that some of this kaolinite must have formed by reaction (1), or by the breakdown of other minerals, such as sanidine or biotite.

The euhedral K-feldspar crystals observed in some assemblage III samples (Figure 4a) may also have formed during the metamorphic event, but only a few samples were examined by SEM, so the presence of such feldspar in assemblage I or II bentonites cannot be ruled out. Similar K-feldspar reported by Sheppard and Gude (1969) from zeolitically altered tuffs of the Barstow Formation was said to have formed by the low temperature alteration of analcime and clinoptilolite; a similar origin may hold for Tulameen.

RELATION OF MINERALOGY TO COAL RANK

Vitrinite reflectance measurement

The coal rank of 45 samples (Figure 3) was estimated (Stach *et al.*, 1975) by measuring maximum percent reflectance in oil ($\bar{R}_0$) of vitrinite in polished pellets of crushed coal; details are given in Williams (1978) and Williams and Ross (1979). Figure 10 shows a plot of $\bar{R}_0$ vs. sample location. The reflectance values in Figure 10 show little variation within each site, but gradually increase from 0.62% in the north to 0.86% in the south. According to the ASTM classification (Bostick, 1979), these coals range in rank from high volatile C bituminous to high volatile A bituminous. It is clear that the thermal event postulated to have formed assemblage III is represented by high reflectance values in the southern part of the basin.

A number of workers have correlated coal and phytoclast rank ($\bar{R}_0$, % VM, BTU content) with the formation of authigenic silicate minerals (e.g., Kisch, 1968; Srodoń, 1979; Castano and Sparks, 1974), but most of these studies were made on coals of higher rank than those at Tulameen and are, therefore, not comparable. For example, Środoń's lowest $\bar{R}_0$ measurement was 0.8%, which is the highest measured in this study; at this value his bentonites contained a mixed-layer clay with about 60% illite layers, which is close to the 55% (K-rectorite) of this study at the same $\bar{R}_0$ value.

Table 4. Paleotemperature as determined from vitrinite reflectance measurements ($\bar{R}_0$).

	Paleotemperature	
$\bar{R}_0$ (Tulameen)	Castano and Sparks (1974), Figure 6.	Bostick (1979), Table 4.
Minimum (0.60%)	75°–130°C	125°C
Smectite → K-rectorite (0.70%)	100°–160°C	145°C
Maximum (0.86%)	130°–200°C	180°C

Estimation of burial temperatures

Attempts have been made to relate $\bar{R}_0$ to paleotemperature since, as pointed out by Bostick (1979), $\bar{R}_0$ is influenced only by temperature and time and, therefore, is a better indicator of temperature than are silicate minerals, which are also affected by rock and fluid composition. The time factor is particularly troublesome, because the same $\bar{R}_0$ could be produced by long heating at low temperature as by short heating at higher temperature.

Both Castano and Sparks (1974) and Bostick (1979) provided charts which relate $\bar{R}_0$ to paleotemperature. These charts are partly based on $\bar{R}_0$ and temperature values obtained from drill holes where the present temperature is thought to be close to the maximum paleotemperature. The temperatures obtained from these data are, therefore, minimum paleotemperatures. Table 4 shows the application of these data to the Tulameen $\bar{R}_0$ values. The dual values shown for the Castano and Sparks (1974) data are for coalification times of 50 and 10 m.y., i.e., 75°C for 50 m.y. would produce the same coal rank as 130°C for 10 m.y. Because the Tulameen coals are thought to have been subjected to a period of hydrothermal metamorphism that was short compared to their 50 m.y. age, the higher values are probably more meaningful. The temperatures from Bostick's data are minimum temperatures.

Table 4 and Figure 10 show that assemblages I and II were stable up to ~145–160°C at which temperature smectite was converted to K-rectorite. The maximum temperature reached was no greater than 200°C. These temperatures can be compared with temperature and mineral data from drill holes in active geothermal areas, where sediments commonly contain silicic glass that

https://doi.org/10.1346/CCMN.1980.0280401 Published online by Cambridge University Press

has altered to clay minerals. Keith *et al.* (1978), Muffler and White (1969), and Steiner (1968) indicated the thermal stability of dioctahedral smectite to be ~100–150°C, and the maximum stability of kaolinite to be ~175°C. Steiner (1968) noted the formation of a rectorite-like mineral at ~200°C. These temperatures, like those at Tulameen, are somewhat higher than those suggested by Perry and Hower (1970) and Hoffman and Hower (1979) for burial metamorphic sequences; but this is to be expected because under burial metamorphic conditions the reaction times are longer, and slow reactions will proceed farther at a lower temperature. In the Gulf Coast geosyncline, Perry and Hower (1970) observed the formation of regularly interstratified illite/smectite at ~100°C, and Hoffman and Hower (1979) suggested that rectorite-type ordering forms between 100 and 175°C; at higher temperature a Kalkberg (ISII) superlattice is formed.

SUMMARY AND CONCLUSIONS

1. Glassy rhyolite tephra which fell into an Eocene coal swamp at Tulameen, British Columbia, first altered to smectite-cristobalite-clinoptilolite or smectite-kaolinite. A later hydrothermal event metamorphosed the smectite to K-rectorite.
2. During the initial alteration of glass, Na was lost from the system.
3. The source of K for the reaction of smectite to K-rectorite was the dissolution of sanidine phenocrysts and possibly other K-bearing phases.
4. Vitrinite reflectance measurements indicate that the smectite was stable to 145–160°C, at which temperature it transformed to K-rectorite.
5. The absence of randomly interlayered illite/smectite intermediate phases suggests a steep thermal gradient, probably related to local magmatism.
6. Tulameen appears to be a hydrothermal example of the burial metamorphic sequence: smectite → interstratified illite/smectite → illite, proposed by Dunoyer de Segonzac (1970).
7. The varying amounts of kaolinite (up to 100%) in individual bentonite beds are probably the result of leaching of alkalies and silica in the acid swamp environment. These kaolinitic bentonites are similar to rocks elsewhere described as tonstein, which also may have a volcanic source.
8. Five subassemblages—smectite-zeolite-cristobalite; smectite-cristobalite; smectite; smectite-kaolinite; and kaolinite—can be recognized within assemblages I and II and may represent assemblages stable at successively lower pH and/or increased leaching as acid swamp waters reacted to varying degrees with the glassy tephra. Such a sequence is supported by activity diagrams of Helgeson *et al.* (1969) and Davies *et al.* (1979).

ACKNOWLEDGMENTS

We thank D. Pearson and D. Grieve, Coal Division, British Columbia Ministry of Mines and Petroleum Resources, for their help with vitrinite reflectance measurements, and T. Adamson of Cyprus Anvil Mining Corporation for guidance in the field and access to cores, trenches, and data. J. W. Sprague, R. Schoonover, S. K. Cruver, T. Sherer, C. A. Ross, J. Roley, K. Shoemaker, P. Combs, and J. Ullin of Western Washington University contributed to various aspects of laboratory analysis, interpretation, computer programming, and manuscript preparation.

REFERENCES

Bohor, B. F., Pollastro, R. M., and Phillips, R. E. (1978) Mineralogical evidence for the volcanic origin of kaolinitic partings (tonstein) in Upper Cretaceous and Tertiary coals of the Rocky Mountain Region: in *Program and Abstracts, 15th Annual Meeting, Clay Minerals Soc.*, Bloomington, Indiana, p. 47.

Bostick, N. H. (1979) Microscopic measurement of the level of catagenesis of solid organic matter in sedimentary rocks to aid exploration for petroleum and to determine former burial temperatures—A review: in *Aspects of Diagenesis,* P. A. Scholle and P. R. Schluger, eds., *Soc. Econ. Paleontol. Mineral. Spec. Publ.* **26,** 17–43.

Bramlette, M. N. and Posnjak, E. (1933) Zeolite alteration of pyroclastics: *Amer. Mineral.* **18,** 492–493.

Castano, J. R. and Sparks, D. M. (1974) Interpretation of vitrinite reflectance measurements in sedimentary rocks and determination of burial history using reflectance and authigenic minerals: in *Carbonaceous Materials as Indicators of Metamorphism,* R. R. Dutcher, ed., *Geol. Soc. Amer. Spec. Pap.* **153,** 31–53.

Davies, D., Almon, W. R., Bonis, S. B., and Hunter, B. E. (1979) Deposition and diagenesis of Tertiary–Holocene volcaniclastics, Guatemala: in *Aspects of Diagenesis,* P. A. Scholle and P. R. Schluger, eds., *Soc. Econ. Paleontol. Mineral. Spec. Publ.* **26,** 281–306.

Davis, G. A. (1977) Tectonic evolution of the Pacific Northwest from Precambrian to present: *WNP-1/4, PSAR, Amendment 23, Subappendix 2RC* (report to the Nuclear Regulatory Commission), Washington Public Power Supply Systems, 46 pp.

Deffeyes, K. S. (1959) Zeolites in sedimentary rocks: *J. Sediment. Petrology* **29,** 602–609.

Dickinson, W. R. (1979) Cenozoic plate tectonic setting of the Cordilleran region in the United States: in *Cenozoic Paleogeography of the Western United States,* J. M. Armentrout, M. R. Cole, and H. TerBest, Jr., eds., Pacific Coast Paleogeography Symp. 3, Pacific Section, Soc. Econ. Paleontol. Mineral. 1–13.

Divis, A. F. and McKenzie, J. A. (1975) Experimental authigenesis of phyllosilicates from feldspathic sands: *Sedimentology* **22,** 147–155.

Dunoyer de Segonzac, G. (1970) The transformation of clay minerals during diagenesis and low grade metamorphism: A review: *Sedimentology* **15,** 281–346.

Eberl, D. D. (1978a) Reaction series for dioctahedral smectites: *Clays & Clay Minerals* **26,** 327–340.

Eberl, D. D. (1978b) The reaction of montmorillonite to mixed-layer clay: The effect of interlayer alkali and alkaline earth cations: *Geochim. Cosmochim. Acta* **42,** 1–7.

Hay, R. L. (1978) Geologic occurrence of zeolites: in *Natural*

Zeolites: Occurrence, Properties, Use, L. B. Sand and F. A. Mumpton, eds., Pergamon Press, Elmsford, N.Y., 135–145.

Hein, J. R., Scholl, D. W., Barron, J. A., Jones, M. G., and Miller, J. (1978) Diagenesis of late Cenozoic diatomaceous deposits and formation of the bottom simulating reflector in the southern Bering Sea: *Sedimentology* **25,** 155–181.

Helgeson, H. C., Brown, T. H., and Leeper, R. H. (1969) *Handbook of Theoretical Activity Diagrams Depicting Chemical Equilibria in Geologic Systems Involving an Aqueous Phase at One Atm. and 0° to 300°C:* Freeman, Cooper and Company, San Francisco, Calif., 253 pp.

Henderson, J. H., Jackson, M. L., Syers, J. K., Clayton, R. N., and Rex, R. W. (1971) Cristobalite authigenic origin in relation to montmorillonite and quartz origin in bentonites: *Clays & Clay Minerals* **19,** 229–238.

Hills, L. V. and Baadsgaard, H. (1967) Potassium-argon dating of some lower Tertiary strata in British Columbia: *Bull. Can. Petrol. Geol.* **15,** 138–149.

Hoffman, J. and Hower, J. (1979) Clay mineral assemblages as low grade metamorphic geothermometers: Application to the thrust faulted disturbed belt of Montana, U.S.A.: in *Aspects of Diagenesis,* P. A. Scholle and P. R. Schluger, eds., *Soc. Econ. Paleontol. Mineral. Spec. Publ.* **26,** 55–79.

Horton, D. G. (1978) *Clay Mineralogy and Origin of the Huntingdon Fire Clays on Canadian Sumas Mountain, Southwest British Columbia:* M.Sc. thesis, Western Washington University, Bellingham, Washington, 96 pp. (unpublished).

Hower, J., Eslinger, E. V., Hower, M. E., and Perry, E. A. (1976) Mechanism of burial metamorphism of argillaceous sediment: 1. Mineralogical and chemical evidence: *Geol. Soc. Amer. Bull.* **87,** 725–737.

Iijima, A. (1978) Geological occurrences of zeolite in marine environments: in *Natural Zeolites: Occurrence, Properties, Use:* L. B. Sand and F. A. Mumpton, eds., Pergamon Press, Elmsford, N.Y., 175–198.

Jackson, M. L. (1974) *Soil Chemical Analysis—Advanced Course.* 2nd Ed., 9th printing: Published by the author, Dept. of Soil Science, Univ. of Wisconsin, Madison, Wisc., 895 pp.

Jones, J. B. and Segnit, E. R. (1971) The nature of opal I. Nomenclature and constituent phases: *J. Geol. Soc. Aust.* **18,** Part I, 57–67.

Keith, T. E., White, D. E., and Beeson, M. H. (1978) Hydrothermal alteration and self-sealing in Y-7 and Y-8 drill holes in northern part of Upper Geyser Basin, Yellowstone National Park, Wyoming: *U.S. Geol. Surv. Prof. Pap.* **1054-A,** 1–26.

Kisch, H. J. (1968) Coal-rank and burial-metamorphic mineral facies: in *Advances in Organic Geochemistry:* P. A. Schenk and I. Havenaar, eds., Pergamon Press, Elmsford, N.Y., 407–425.

Loughnan, F. C. (1978) Flint clays, tonsteins and the kaolinite clayrock facies: *Clay Miner.* **13,** 387–400.

MacEwan, D. M. (1956) Fourier transform methods for studying scattering from lamellar systems. I. A direct method for analysing interstratified mixtures: *Kolloid Z.* **149,** 96–108.

Mueller, R. F. and Saxena, S. K. (1977) *Chemical Petrology:* Springer-Verlag, New York, 394 pp.

Muffler, P. and White, D. E. (1969) Active metamorphism of Upper Cenozoic sediments in the Salton Sea Geothermal Field and the Salton Trough, southeastern California: *Geol. Soc. Amer. Bull.* **80,** 157–182.

Mumpton, F. A. (1960) Clinoptilolite redefined: *Amer. Mineral.* **45,** 351–369.

Murata, K. J. and Whiteley, K. R. (1973) Zeolites in the Miocene Briones Sandstone and related formations of the Central Coast Ranges, California: *J. Res. U.S. Geol. Surv.* **1,** 255–265.

Okulitch, A. V., Price, R. A., and Richards, T. A. (1977) A guide to the geology of the southern Canadian Cordillera: *Geol. Assoc. Can.-Mineral. Assoc. Can.-Soc. Econ. Geol. Field Trip Guidebook* **8,** 135 pp.

Perry, E. A. and Hower, J. (1970) Burial diagenesis in Gulf Coast pelitic sediments: *Clays & Clay Minerals* **18,** 165–177.

Reynolds, R. C., Jr. (1967) Interstratified clay systems: Calculation of the total one-dimensional diffraction function: *Amer. Mineral.* **52,** 661–672.

Reynolds, R. C., Jr. and Anderson, D. M. (1967) Cristobalite and clinoptilolite in bentonite beds of the Colville Group, northern Alaska: *J. Sediment. Petrology* **37,** 966–969.

Reynolds, R. C., Jr. and Hower, J. (1970) The nature of interlayering in mixed-layer illite-montmorillonite: *Clays & Clay Minerals* **18,** 25–36.

Sheppard, R. A. and Gude, A. J., 3rd (1969) Diagenesis of tuffs in the Barstow Formation, Mud Hills, San Bernardino County, California: *U.S. Geol. Surv. Prof. Pap.* **634,** 36 pp.

Spears, D. A. and Kanaris-Sotiriou, R. (1979) A geochemical and mineralogical investigation of some British and other European tonsteins: *Sedimentology* **26,** 407–425.

Środoń, J. (1979) Correlation between coal and clay diagenesis in the Carboniferous of the Upper Silesian Coal Basin: in *International Clay Conference 1978,* M. M. Mortland and V. C. Farmer, eds., Elsevier, Amsterdam, 251–260.

Środoń, J. (1980) Precise X-ray identification of illite/smectites: *Clays & Clay Minerals* **28,** (in press).

Stach, E., MacKowsky, M. Th. Teichmuller, M., Taylor, G. H., Chandra, D., and Teichmuller, R. (1975) *Stach's Textbook of Coal Petrology:* Gebruder Borntraeger, Berlin, 398 pp.

Steiner, A. (1968) Clay minerals in hydrothermally altered rocks at Wairakei, New Zealand: *Clays & Clay Minerals* **16,** 193–213.

Thompson, G., Fields, R. W., and Alt, D. (1978) Major Tertiary climate variations in the western United States as indicated by paleosol mineralogy and sedimentation patterns: in *Program and Abstracts, 15th Annual Meeting, Clay Minerals Soc.,* Bloomington, Indiana, p. 35.

Williams, V. E. (1978) *Coal Petrology of the Tulameen Coalfield, South-Central British Columbia:* M.Sc. thesis, Western Washington University, Bellingham, Washington, 77 pp. (unpublished).

Williams, V. E. and Ross, C. A. (1979) Depositional setting and coal petrology of Tulameen Coalfield, South-Central British Columbia: *Amer. Ass. Petrol. Geol. Bull.* **63,** 2058–2069.

Wright, T. L. (1968) X-ray and optical study of alkali feldspar—Pt. 2: *Amer. Mineral.* **53,** 88–104.

(Received 3 December 1979; accepted 12 March 1980)

Резюме—Туламинский угольный бассейн является частью эоценового континентального бассейна, в который поступило большое количество вулканокластических отложений из-за его расположения в активном магматическом поясе. Бентонитовые прослои в угле первоначально состояли из стекловидной виолитовой тефры с фенокристаллами санидина, биотита, и кварца. Во время первоначального изменения, которое происходило в болотных условиях или вскоре после захоронения, стекло преобразовалось в смектит-кристобалит-клиноптилолит или в смектит-каолинит. Образование каолинита зависело от степени выщелачивания кремнезема и шелочей в болотной среде. Некоторые пласты состоят почти на 100% из каолинита и могут быть определены как тонштейн. Смектит является бейделлитовым и не проявляет признаков переслаивания; каолинит хорошо упорядочен. Во время изменения натрий, который первоначально входил в состав стекла, был удален из системы.

Позднее какое-то термическое событие, которое повлияло только на южную часть бассейна, превратило смектит в равномерно переслаивающийся иллит-смектит с 55% иллитовых слоев и сверхструктурой ректоритового типа (тип IS). Источником калия служило растворение санидина. Измерения витринитовых отражений угля показывают, что смектит был стойким до температур 145–160°C, при которых он превращался в К-ректорит. Отсутствие беспорядочно переслаивающихся промежуточных звеньев даже в богатых калием пластах указывает на то, что преобразование смектита в К-ректорит было обусловлено значительным термальным градиентом, возможно происшедшим из-за местного магматизма или циркуляции геотермальных растворов. [N.R.]

Resümee—Das Kohlengebiet von Tulameen ist Teil eines eozänen, nichtmarinen Beckens, das aufgrund seiner Lage in einem aktiven Magmenbogen sehr viele vulkanoklastische Sedimente enthält. Die Bentonitanteile in der Kohle waren ursprünglich glasige, rhyolithische Tephra mit Einsprenglingen von Sanidin, Biotit, und Quarz. Zu Beginn der Umwandlung, die im Schlamm oder kurz nach der Überdeckung stattfand, wurde das Glas entweder in Smektit-Cristobalit-Klinoptilolit oder in Smektit-Kaolinit umgewandelt. Die Bildung von Kaolinit hängt vom Auslaugungsgrad des SiO_2 und der Alkalien im Schlamm ab. Einige Lagen bestehen aus nahezu 100% Kaolinit und können als Tonstein bezeichnet werden. Der Smektit ist beidellitisch und zeigt keine Anzeichen von Zwischenlagen; der Kaolinit ist gut geordnet. Während der Umwandlung ging Natrium, das ursprünglich eine Komponente des Glases war, aus dem System verloren.

Ein späteres thermales Ereignis, das nur den südlichen Teil des Beckens betraf, wandelte den Smektit in eine reguläre Wechsellagerung Illit-Smektit um, mit 55% Illitlagen und einem Gitter vom Rektorittyp (IS-Typ). Das Kalium kam von der Auflösung des Sanidins. Messungen des Reflexionsvermögens am Vitrinit der Kohle deuten darauf hin, daß der Smektit bis zur Temperatur zu 145°–160°C stabil war, bei der er in K-Rektorit umgewandelt wurde. Das Fehlen von Übergangsphasen mit unregelmäßigen Wechsellagerungsstrukturen, selbst in den Kalium-reichen Lagen, deutet darauf hin, daß die Umwandlung von Smektit in K-Rectorit durch einen steilen thermischen Gradienten bestimmt wurde, der möglicherweise mit einem lokalen Magnetismus oder mit zirkulierenden geothermalen Lösungen zusammenhängt. [U.W.]

Résumé—Le champ charbonnier Tulameen fait partie d'un bassin non marin éocien qui recevait des sédiments volcaniclastiques extensifs dûs à son emplacement dans un arc magmatique actif. Des délitations de bentonite dans le charbon consistaient originalement de tephra vitreux rhyolitiques avec des phénocrystes de sanidine, de biotite, et de quartz. Pendant la période initiale d'altération, qui s'est deroulée dans le marais ou peu après enterrement, le verre a été transformé soit en de la smectite–cristobalite–clinoptilolite, soit en de la smectite–kaolinite. La formation de kaolinite dépendait du degré de lessivage de la silice et des alcalins dan l'environement marécageux. Certains lits sont presque 100% kaolinite et pourraient être designés tonstein. La smectite est beidellitique et ne montre aucune évidence d'interstratification, la kaolinite est bien ordonnée. Pendant l'altération, le système a perdu le sodium, originalement un composé du verre.

Un évenement thermique subséquent, qui n'a affecté que la partie sud du bassin, a metamorphosé la smectite en une illite/smectite régulièrement interstratifiée avec 55% de couches d'illite et un super-réseau du type rectorite (type IS). La source du potassium était la dissolution de sanidine. Des mesures de réflectance de vitrinite du charbon suggèrent que la smectite était stable jusqu'à 145°–160°C, température à laquelle elle a été transformée en rectorite-K. L'absence d'intermédiaires interstratifiés au hasard suggère que la transformation de smectite en rectorite-K était controllée par un gradient thermique résultant possiblement d'un magmatisme local ou de fluides géothermiques circulants. [D.J.]